Molecular Neurobiology (2019) 56:8435–8450
https://doi.org/10.1007/s12035-019-01682-x

# Early Sociability and Social Memory Impairment in the A53T Mouse Model of Parkinson's Disease Are Ameliorated by Chemogenetic Modulation of Orexin Neuron Activity

Milos Stanojlovic [1] · Jean Pierre Pallais Yllescas Jr [1] · Aarthi Vijayakumar [1] · Catherine Kotz [1,2]

Received: 16 April 2019 / Accepted: 14 June 2019 / Published online: 27 June 2019


## Abstract

Parkinson's disease (PD) is a multi-layered progressive neurodegenerative disease. Signature motor system impairments are accompanied by a variety of other symptoms such as mood, sleep, metabolic, and cognitive disorders. Interestingly, social cognition impairments can be observed from the earliest stages of the disease, prior to the onset of the motor symptoms. In this study, we investigated age-related reductions in sociability and social memory in the A53T mouse model of PD. Since inflammation and astrogliosis are an integral part of PD pathology and impair proper neuronal function, we examined astrogliosis and inflammation markers and parvalbumin expression in medial pre-frontal cortex (mPFC), part of the brain responsible for social cognition regulation. Finally, we used DREADDs (Designer Receptors Exclusively Activated by Designer Drugs) for the stimulation and inhibition of orexin neuronal activity to modulate sociability and social memory in A53T mice. We observed that social cognition impairment in A53T mice is accompanied by an increase in astrogliosis and inflammation markers, in addition to loss of parvalbumin neurons and inhibitory pre-synaptic terminals in the mPFC. Moreover, DREADD-induced activation of orexin neurons restores social cognition in the A53T mouse model of PD.

## Significance Statement

Social cognition is severely affected in the early stages of Parkinson's disease. In this study, we identified the A53T mouse as a model of social cognitive impairment in PD. Observed alterations in sociability and social memory are accompanied by loss of parvalbumin positive neurons and loss of inhibitory input to mPFC. Stimulating orexin neurons using a chemogenetic approach (DREADDs) ameliorated social cognitive impairment. This study identifies a role for orexin neurons in social cognition in PD and suggests potential therapeutic targets for PD-related social cognition impairments.

**Keywords** Parkinson's disease · Orexin · Social cognition · Neuromodulation · mPFC

## Introduction

Parkinson's disease (PD) is the second most common neurodegenerative disease, affecting 2–3% of the population over 65 years of age [1]. Originally, dopamine deficiency caused by dopamine neuron loss in the substantia nigra, presence of Lewy bodies, and movement disorder were considered hallmarks of PD. Today, PD is recognized as a complex, multifactorial disease. Studies have shown that PD affects different neuronal populations [1, 2] and mood, cognition, and metabolism before the onset of the signature motor impairments [3–6].

Orexin (hypocretin) is a neurotransmitter predominantly produced in a subpopulation of neurons located in the lateral hypothalamus (LH). Original studies from Sakurai [7] and Yoshida [8] identified complex projection patterns of these neurons. Initial studies investigating the role of orexin addressed hypothalamic-regulated physiological functions [9–14]. In time, a significant amount of data accumulated demonstrating orexin's role in other processes including mood, cognition, stress, anxiety, and pain [15–21]. Several studies suggest that orexins contribute to PD pathology.

✉ Milos Stanojlovic
milosmolbio@gmail.com

[1] Integrative Biology and Physiology, University of Minnesota, Minneapolis, MN, USA

[2] GRECC, Minneapolis VA Health Care System, Minneapolis MN, USA

Sleep impairments occur relatively early in PD progression and are associated with orexin circuitry dysfunction [22, 23], and reductions of orexin in cerebrospinal fluid and orexin neuronal losses are detected in advanced stages of PD [22–25].

Prefrontal cortex (PFC) is a brain region critical in mediating social cognition [26]. It is believed that medial PFC (mPFC) is responsible for processing contextual social cues to guide social complex behaviors [26–28] that require internal social processing of both self and other; such behaviors include empathy, mentalizing, self-reflection, and personal moral reasoning [29, 30]. Interestingly, not only do orexin neurons project from LH to PFC [7, 8, 31], orexin receptors are present in PFC, and orexin is a strong modulator of mPFC function. Studies confirmed that orexin inputs can excite PFC neurons through both direct and indirect mechanisms inducing improvements in attention, short term and spatial memory [32–35]. Furthermore, acute intranasal administration of orexin A induces the immediate early gene expression of c-Fos, a marker for neuronal activation, in the PFC, increasing both ACh and glutamate efflux in this region [36]. Parkinson's disease studies report functional, neuroanatomical, and pathological changes in PFC of PD patients [37, 38] accompanied by impairment in social cognition from the earliest stages of the disease [39, 40].

The Hualpha-Syn (A53T) transgenic line G2-3 (A53T mice) express the familial PD-associated A53T missense mutant form of human α-syn under the control of the PrP promoter (murine prion promoter). Compared to other PD transgenic mouse models, A53T mice show the complete α-syn pathology that is observed in humans [41] and is extensively studied in the context of neurodegeneration, α-syn aggregation, and toxicity [42]. These mice spontaneously develop the neurodegenerative disease between 9 and 16 months of age with a progressive motoric dysfunction leading to death within 14–21 days of onset [43]. Furthermore, these mice show an interesting behavioral phenotype prior to the disease onset which is characterized by cognitive impairment, hyperactivity, and reduced anxiety-like behavior [42, 44–46].

In the first part of this study, we determined if A53T mice show social cognition impairments. To assess sociability and social memory, we used the three-chamber social interaction test (3CSIT). We observed early changes in sociability and age-dependent social memory impairment. These behavioral changes were accompanied with increases in astrogliosis and inflammatory markers, loss of parvalbumin positive neurons, and a reduction of inhibitory input to the mPFC. Considering that orexin neurons are strong modulators of mPFC function [32–35], in the second part of our study, we hypothesized that modulation of orexin neuron activity will change sociability and social memory in A53T mice. To manipulate the activity of orexin neuronal populations in vivo, we used a chemogenetic tool known as designer receptors exclusively activated by designer drugs (DREADDs). G protein coupled DREADDs use a modified form of the human M3/M4 muscarinic receptor (hM3Dq/ hM4Di) to induce an excitatory/inhibitory cellular response in the presence of their ligand, clozapine-*N*-oxide (CNO). Clozapine-*N*-oxide-induced activation of hM3Dq mobilizes intracellular calcium and increases neuronal excitability, while inhibitory effects of hM4Di stimulation are a result of CNO's stimulation and resulting activation of G protein inwardly rectifying potassium (GIRK) channels. In this part of the study, we investigated if DREADD-induced modulation of orexin neuron activity affects sociability and social memory in A53T mice.

## Materials and Methods

### Animals and Ethics Statement

All experimental procedures in this study were approved by the University of Minnesota Animal Care and Use Committee. Adult male C57BL/6J (wt), A53T, orx-Cre, and orx-Cre/A53T mice were maintained on a 12-h light/dark cycle with chow and water ad libitum. Orx-Cre mice were initially obtained from Prof. Takeshi Sakurai (Kanazawa University, JA) and bred on C57BL/6J background in our colony. Generation and initial phenotyping of orx-Cre and wild-type heterozygous mice was conducted and has been described previously [47, 48]. The A53T mice were generated and characterized as described previously [49], obtained from the Jackson Laboratory (ME, US) and bred on a C57BL/6J background in our colony. Since female A53T mice tend to neglect their litters, orx-Cre/A53T mice were generated by crossing orx-Cre positive females and A53T positive males.

### Three-Chamber Social Interaction Test

The three-chamber social interaction test was used to assess sociability and social memory in mice. The 3CSIT test exploits mouse tendency to spend more time with another mouse as compared to time spent alone in an identical but empty chamber (sociability) and tendency to spend more time investigating a previously un-encountered mouse rather than a familiar one (social memory).

**Equipment and Experimental Setup** A translucent plexiglass apparatus composed of three chambers (individual chamber dimension: 42 × 19 × 22; the whole apparatus: 61 × 42 × 22 (L × W × H, cm)) separated by walls containing removable dividers was used for this test. Two wire cup-like containers large enough to enable free movement of the target mice were used to enable exchange between mice and prevent direct

physical interactions. Room lightning was set to 60 lx. The camera connected to a computer and ANY-maze software (San Diego Instruments, CA) were used to track and analyze the movement in real-time mode. After each trial, chambers were thoroughly cleaned with 70% ethanol. Behavioral tests were performed between 9:00 am and 1:00 pm.

**Animal Preparation** Two types of animals were used in this study: test mice, used in the experiment, and target mice, with which the test mice interact. Target mice were of the same age and background as the test mice and did not have previous contact with them. Two control mice were used per experiment, one as a target animal in the sociability trial and as the familiar animal in social memory trials, and another animal for social memory trials only, to represent the novel animal. Target mice were habituated for wire cup containers 3 days prior the test, first day for 10 min, second day for 15 min, and third for 20 min.

**Three-Chamber Social Interaction Test** All the cages containing target and test mice were transferred to the behavioral room 30 min before the first trial begins. Test mice were i.p. injected with either saline or 3 mg/kg of CNO dissolved in saline 30 min prior to the test.

**Habituation** Wire cups were placed in the middle of the left and right chambers. Test mice were placed in the center chamber for a 5-min habituation period while the other chambers remained inaccessible by dividing plexiglas walls.

**Sociability Trial** Following habituation, one target mouse (stranger 1, S1) was placed inside a wire containment cup that is located in one of the side chambers. The placement of S1 in the left or right chamber is systematically altered between trials. Walls between chambers were removed, allowing free access to both left and right chambers. Animals were observed for 10 min and empty cup (object, O) and S1 interaction time was analyzed. Preference index was calculated using the following formula: preference index = S1 interaction time (s) / O interaction time (s).

**Social Memory Trial** Following the sociability trial, the mouse was placed into the center chamber, but access to the left and right chambers was restricted using plexiglass dividers. In this trial, the S1 mouse acted as a familiar subject and remained in its original position. The second target mouse (stranger 2, S2) was placed inside an identical wire containment cup in the opposite chamber (which remained empty during the sociability trial). Animals were observed for 10 min and S1 and S2 interaction time was analyzed. Preference index was calculated by using the following formula: preference index = S2 interaction time (s) / S1 interaction time (s).

## Viral Injections

Animals were anesthetized with isofluorane (1–4%) and placed in a stereotactic apparatus (Kopf Instruments). DREADD targeting was achieved by stereotaxic injection of a Cre-dependent AAV vector expressing a double-floxed inverted open reading frame (DIO) around the DREADD transcript and a fluorescent tag (mCherry). Vectors (AddGene, MA) were injected into the LH (AP-1.8/DV-5.5/ML ± 0.9 mm from bregma; 333 nl/5 min) [50] of orx-Cre or orx-Cre/A53T mice. Control groups were injected with pAAV-hSyn-DIO-mCherry (AAV8, $2.1 \times 10^{13}$ GC/ml) (cDREADD). Excitatory neuromodulation was achieved via Gq-coupled pAAV-hSyn-DIO-hM3D(Gq)-mCherry (AAV8, $2.5 \times 10^{13}$ GC/ml) (qDREADD). Inhibitory neuromodulation was achieved via Gi-coupled pAAV-hSyn-DIO-hM4D(Gi)-mCherry (AAV8, $1.9 \times 10^{13}$ GC/ml) (iDREADD). Animals recovered from the surgery for 4 weeks and were randomly assigned to appropriate experimental groups prior to testing.

## Immunohistochemistry

Mice were perfused intracardially with ice-cold saline, followed by 20 ml of 4% paraformaldehyde (PFA) in PBS (phosphate-buffered saline). Brains were harvested and post-fixed in 4% PFA/PBS overnight at 4 °C, followed by 30% (*w*/*v*) sucrose in PBS solution at 4 °C until the brains sank. The brains were imbedded in OCT (Optimal Cutting Temperature Compound; Sakura, CA), frozen in dry ice-cooled ethanol, and then immediately cut. Coronal brain sections were collected and stored in cryoprotectant (30% (*w*/*v*) sucrose, 30% (*v*/*v*) ethylene glycol, 1% (*w*/*v*) PVP-40 in PB). Brain sections were washed six times for 5 min with 0.1 M PBS, pH 7.4. Antigen retrieval was performed using Antigen Unmasking Solution (Vector Laboratories, CA). After initial washing, the sections were transferred to Antigen Unmasking Solution and incubated for 30 min at 90 °C. The brain slices were then washed three times for 5 min in PBS and incubated with 5% normal horse serum in PBST (0.01% Tween in PBS) for 2 h at room temperature. After washing three times in PBST, the sections were incubated with primary antibodies (mouse anti-p-α-syn (Alpha-synuclein (phospho S129)), Abcam, MA; rabbit anti-p-α-syn (Alpha-synuclein (phospho S129)), Abcam, MA; rabbit anti-GFAP (glial fibrillary acidic protein), Abcam, MA; guinea pig anti-IBA1 (anti-ionized calcium binding adaptor molecule 1) Novus Biologicals, CO; guinea pig anti-NeuN (neuronal nuclei), MilliporeSigma, MA; guinea pig anti-GAD65 (glutamate decarboxylase), Synaptic Systems, DE; rabbit anti-synaptophysin, Abcam, MA; goat anti-orexin A, Santa Cruz, CA; rabbit c-Fos, Santa Cruz, CA; 1:1000) overnight at RT on

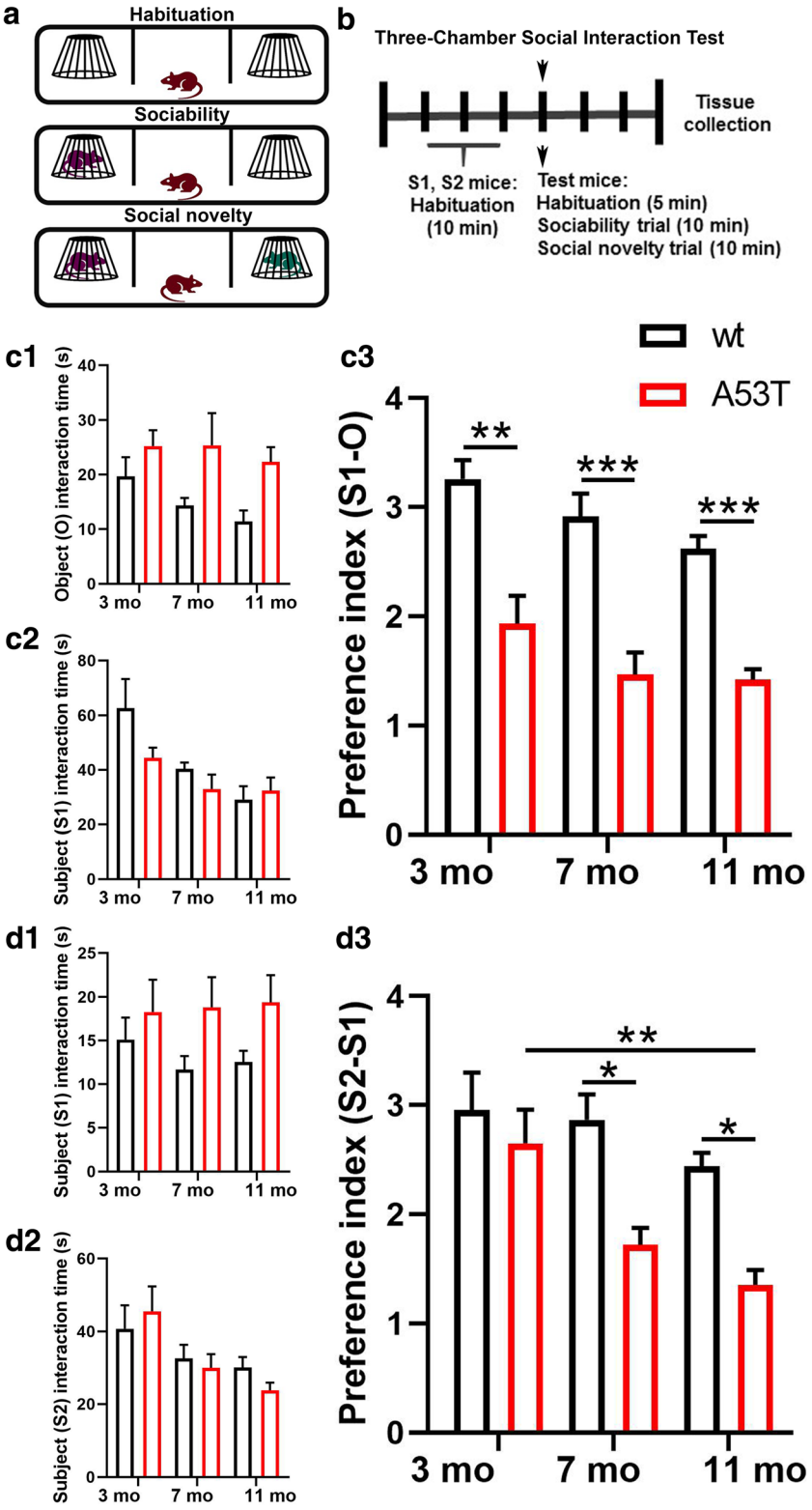


a platform shaker. Brain sections were washed in PBST four times for 10 min after primary antibody incubation and incubated with secondary antibodies conjugated with Alexa Fluor dyes (donkey anti-mouse, donkey anti-rabbit, donkey anti-goat, donkey anti-guinea pig; 1:500, Invitrogen, CA). Brain sections were then washed four times for 10 min in PBST and then mounted with ProLong Gold mounting media (Invitrogen, CA).

◀ **Fig. 1** Sociability and social memory in male 3-, 7-, and 11-month-old wt and A53T mice. Schematic representation of the three-chamber social interaction test (3CSIT) (**a**). The timeline of the experimental procedure (**b**). Mice were subjected to a 3CSIT. Three days following 3CSIT, mice were perfused and brains were collected. Sociability trials: time test mice spend interacting with empty cup (O) (**C1**) and stranger 1 (S1) mouse (**b2**). A reduced (S1-O) preference index can be observed in A53T mice compared to wt animals at 3, 7, and 11 months of age (**c3**). Social memory trials: time the test mice spend interacting with S1 mouse (**d1**) and stranger 2 (S2) mouse (**d2**). A reduced (S2-S1) preference index can be observed in A53T mice compared to wt animals at 7 and 11 (**d3**). Further, aging induced decrease in (S2-S1) preference index can be observed between 3- and 11-month A53T mouse (*D3*) (3 months, $n = 8$/group; 7 months, $n = 7$/group; 11 months, $n = 8$/group; two-way ANOVA, Sidak; $*p < 0.05$, $**p < 0.01$, $***p < 0.005$)

## Immunofluorescence Imaging and Image Analysis

Immunofluorescence images for densitometry and IBA1 positive cell density experiments were captured using the Nikon Eclipse NI-E microscope (Nikon, JA), with a monochrome Nikon Black & White camera DS-QiMc (Nikon, JA). Each fluorochrome is represented as a pseudo-color in the images. For quantification of p-α-syn, GFAP, IBA1, and parvalbumin every 6th coronal section from − 1.34 to 2.34 bregma [50] (four in total) for mPFC (prelimbic area (Pl), the infralimbic area (Il), medial orbital area (Mo), and cingulate cortex area (Cg)). Images were captured (2 per section, 8 per mice) using 10× magnification (z-stacks, 5 μm step). Optical density was determined with image analysis software (Image J, National Institutes of Health) by measuring the mean gray value of the mPFC region of interest (ROI). For IBA and parvalbumin cell density, Z-stack images (5 μm step) were captured using 20× magnification. The IBA positive cell densities in the mPFC region were determined using Image J by counting the positive cells in two areas of the mPFC of every 6th section from 1.34 to 2.34 bregma [50] (eight per mice) and divided by the ROI. For the p-α-syn localization study, every 6th LH section from − 0.94 to − 2.18 bregma [50] (four in total) was stained and analyzed. To determine the percentage of orexin A positive cells containing p-α-syn, every 6th coronal section from − 0.94 to − 2.18 bregma [50] (five in total) was analyzed. Z-stack images (5 μm step) were captured using 10× magnification. To confirm the orexin neuron intracellular p-α-syn localization, Z-stack images (5 μm step) were captured using 40× magnification.

## Unbiased Stereology

Unbiased stereology analysis with optical fractionator probe within the Stereo Investigator 11.1.2 software (MBF Bioscience, VT) was used to quantify the number of orexin A positive cell numbers in LH. Sections were cut at 40 μm to allow for an 18 μm dissector height within each section after dehydration and mounting. Systematic sampling of every third section was collected through the orexin field beginning at bregma − 0.94 and finishing at − 2.18 [50], with the first sampled set of sections chosen at random. Sections were imaged using an Axio Imager M2 fluorescence microscope (Zeiss, DE). Orexin field boundaries were used to outline contours at 5× magnification. Cells were counted using a

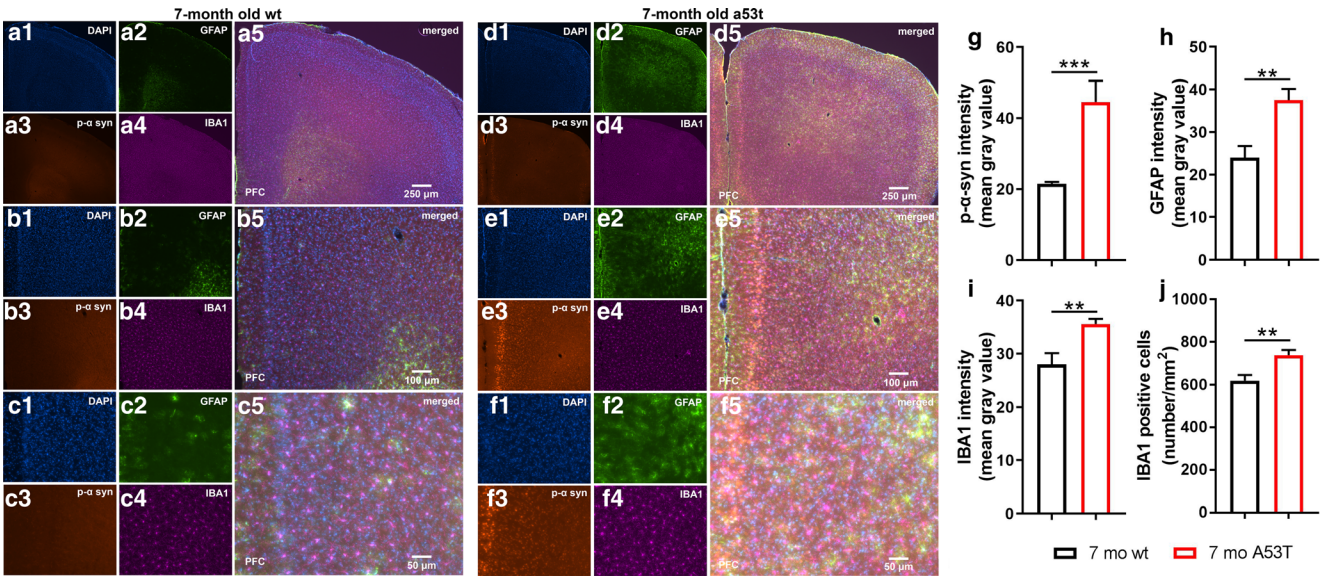


**Fig. 2** Expression of p-α-syn, GFAP, and IBA1 in the mPFC of 7-month-old wt and A53T mice. Representative IF microphotographs of the DAPI, p-α-syn, GFAP, IBA1 and the merged image in 7-month wt mice (**a**–**c**) and A53T mice (**d**–**f**) used for p-α-syn, GFAP, and IBA1 densitometry and IBA1 call density analysis. Image J was used to quantify the intensity of p-α-syn, GFAP, and IBA1 staining and density of IBA1 positive cells. Increased expression of the p-α-Syn (G), GFAP (H), and IBA1 (I) was observed in A53T mice compared to wt mice. The A53T mice showed increased density of IBA1 positive cells (J) (Student's *t* test, $n = 5$/group; $*p < 0.05$, $**p < 0.01$)

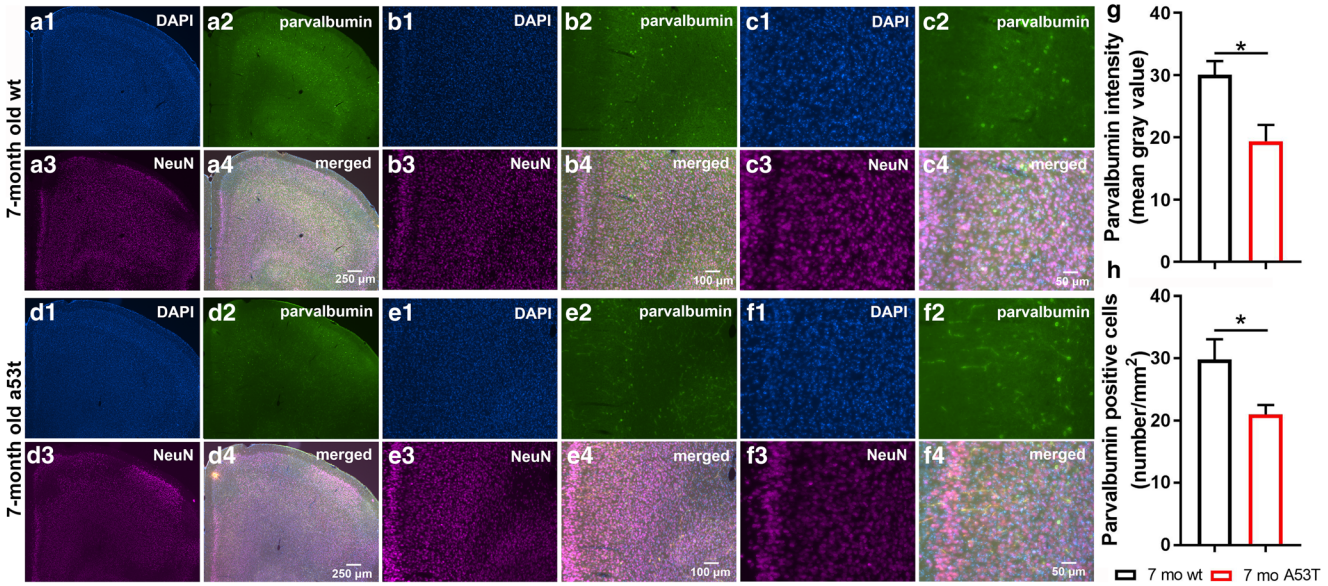


**Fig. 3** Parvalbumin positive cell density and expression in the mPFC of 7-month-old wt and A53T mice. Representative IF microphotographs of DAPI, parvalbumin, NeuN and merged images in 7-month wt (**a**–**c**) and A53T mice (**d**–**f**). Image J was used to quantify the intensity of parvalbumin and and density of parvalbumin positive cells. Decreased expression of parvalbumin (**g**) was observed in A53T mice compared to wt mice. The A53T mice showed reduced density of parvalbumin positive cells (**h**) (Student's *t* test, $n = 5$/group; $^{*}p < 0.05$, $^{**}p < 0.01$)

randomly positioned grid system controlled by Stereo Investigator in a previously defined region in all optical planes. Guard zones were set at 10% of the section thickness to account for damage during the staining procedure. The grid size was set to 100 × 100 μm and the counting frame to 80 × 80 μm. Counting was performed at 63× magnification (oil). The average coefficient of error (CE, m = 1) ratio for all of the mice imaged was 0.085. Neurons were counted throughout the entire orexin field of a single hemisphere of each mouse to give an acceptable coefficient of error (CE) (Gunderson method) of 0.1 using the smoothness factor m = 1. The CE provides a means to estimate sampling precision, which is independent of natural biological variance. As the value approaches 0, the uncertainty in the estimate precision reduces. CE = 0.1 is deemed acceptable within the field of stereology. Cells were only counted if they touched the inclusion border or did not touch the exclusion border of the sampling grid.

## Quantification of Pre-synaptic Inhibitory Terminals

Quantification of inhibitory pre-synaptic terminals was performed using an immunocytochemistry-based assay and puncta analyzer image J plugin [51, 52]. Three independent coronal brain sections for each mouse (16 μm thick, 3 images per section), containing the mPFC (bregma 1.43–2.10 mm) [53] were stained with GAD65 (glutamate decarboxylase, 65 kDa isoform localized predominantly in synaptic terminals) and synaptophysin (presynaptic protein associated with small synaptic vesicles). The 5-μm-thick confocal scans (optical section depth 0.33 m, 15 sections/scan of the mPFC) were performed at 60× magnification on a Nikon C2 Automated Upright Widefield and Confocal Microscope (Nikon, JP). Maximum projections of three consecutive optical sections (corresponding to 1 μm total depth) were generated. The Puncta Analyzer Plugin for ImageJ, image analysis software (National Institutes of Health) was used to count the number of colocalized pre-synaptic markers. Details of the quantification method using puncta analyzer plugin were given by Ippolito and Eroglu (2010) [52].

## Statistical Analyses

All data were analyzed using either Prism 6.0 (GraphPad Software, CA) or SPSS (IBM, NY). Statistical analyses of phenotyping behavioral data were performed using a two-way ANOVA followed by Sidak's post hoc analysis. Statistical analyses of DREADD behavioral data were performed using a one-way ANOVA followed by Tukey's post hoc analysis. Densitometry, cell, and pre-synaptic terminals count data were analyzed using Student's *t* test.

## Experimental Design and Exclusion Criteria

The initial phenotyping study was performed in male 3, 7, and 11-month old wt and A53T mice. Animal numbers used in 3CSIT were as follows: 3 months, $n = 8$/group; 7 months, $n = 7$/group; 11 months, $n = 8$/group. Three days following 3CSIT, the animals were sacrificed, and their brains were collected for analysis. Seven-month-old mice in the phenotyping study ($n = 5$ per group) were used for

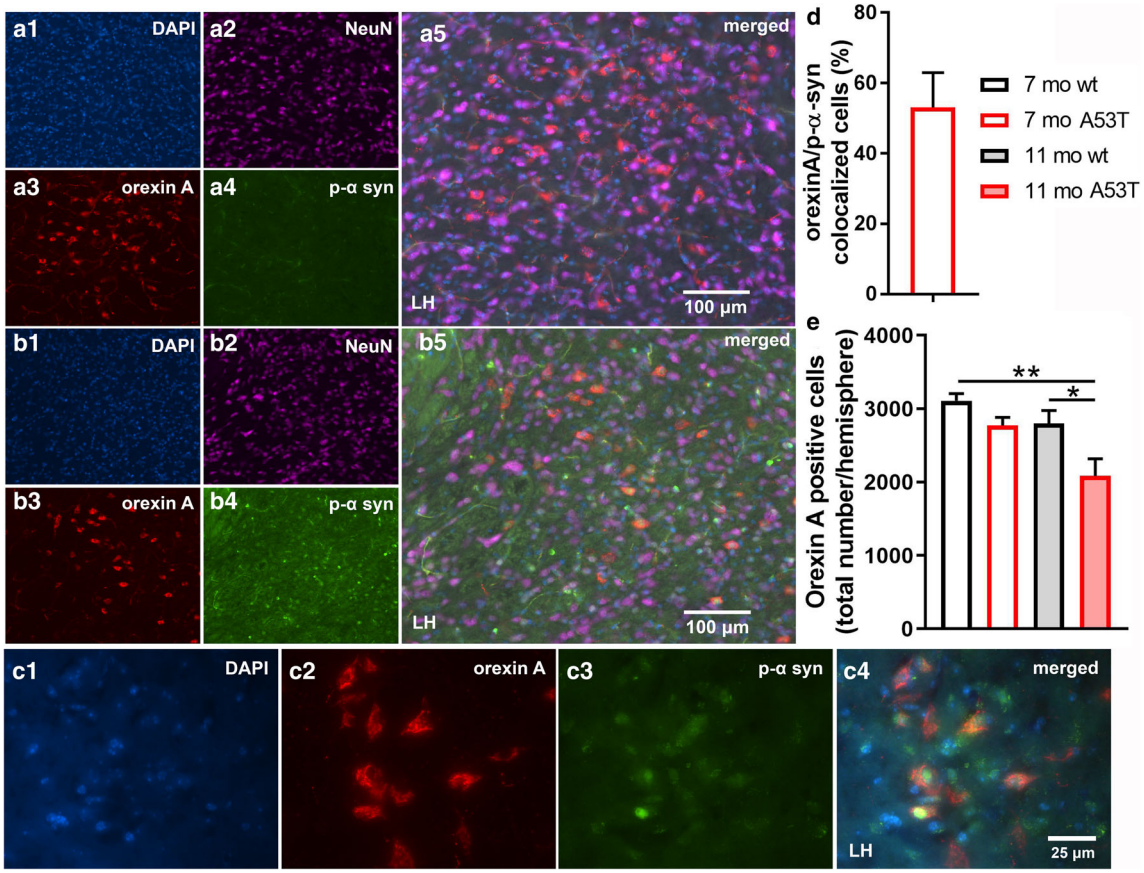


**Fig. 4** Immunofluorescence (IF) analysis of p-α-syn expression in orexin neurons and number of orexin neurons. Representative IF microphotographs of the DAPI, NeuN, orexin A, p-α-syn, and merged image in 7-month wt (**a**) and A53T mice (**b**), showing a lack of p-α-syn expression in 7-month wt mice and presence of p-α-syn in the orexin field of 7-month A53T mice. **c** Representative IF microphotographs of the orexin A, p-α-syn, and merged image in 7-month A53T mice (**c**) showing the presence of the p-α-syn in the orexin neurons. **d** Percentage of orexin neurons expressing p-α-syn defined as orexin A/p-α-syn colocalized cells in 7-month A53T mice. Unbiased stereology analysis showed reduced number of the orexin A positive neurons between 11-month wt and A53Tmice and between 7-month wt and 11-month A53T mice (**e**) (Student's *t* test, $n = 4$/group; $^{*}p < 0.05$, $^{**}p < 0.01$)

IHC analysis, in which every 6th coronal section containing mPFC 1.34 to 2.34 or LH bregma 0.94 to − 2.18 bregma was collected, stained, and analyzed. For the unbiased stereology study, every third section from − 0.94 to − 2.18 bregma was collected and analyzed using the Stereo Investigator 11.1.2 software. Seven- and 11-month old wt and A53T animals were used for the unbiased stereology analysis ($n = 4$/group). For pre-synaptic inhibitory terminal quantification, three mice/groups were used.

CNO effects on social cognition studies were tested in 7-month orx-Cre mice with viral intracranial injections containing the cDREADD. After a 2-week recovery period, animals were introduced to the behavioral 3CSIT. Mice were i.p. injected with either saline or 3 mg/kg of CNO dissolved in saline 30 min prior to the test ($n = 6$/group). Three independent coronal brain sections per each mouse (three images per section, nine total) were analyzed.

The DREADD study was performed in male 7-month orx-Cre and orx-Cre/A53T animals subjected to viral intracranial injections containing either the cDREADD, qDREADD, or iDREADD constructs. After a 2-week recovery period, animals were introduced to the behavioral 3CSIT. Mice were injected with 3 mg/kg of CNO dissolved in saline 30 min prior to the test. The animal numbers used in the 3CSIT were as follows: orx-Cre with cDREADD, $n = 8$; orx-Cre/A53T with cDREADD, $n = 8$; orx-Cre/A53T with qDREADD, $n = 8$; orx-Cre/A53T with iDREADD, $n = 9$. Three days following the 3CSIT, the animals were sacrificed, and their brains collected for analysis (Fig. 4a). All animals used in the DREADD study were perfused, and their brains were collected for injection placement confirmation. Coronal sections containing LH from − 0.94 to − 1.94 bregma were collected and analyzed. Animals were excluded from the experiment if post hoc histological analyses showed inaccurate viral injection placement. Mice were observed for neurological deficits and underperformance in behavioral tests, although none were observed. For DREADD expression analyses, all animals were observed, while for c-Fos analyses, qDREADD subjects were

i.p. injected with either saline or CNO (5 mg/kg) 90 min prior to perfusion to confirm functional activation of the DREADD in orexin neurons by c-Fos (immediate early gene) labeling. Every sixth coronal section containing LH from − 0.94 to − 1.94 bregma ($n = 5$ per group) was stained for orexin A and c-Fos and then analyzed.

## Results

### Socialization and Social Memory Impairment in a A53T Mouse Model of PD

To characterize socialization and social memory, we used 3-, 7-, and 11-month-old (mo) wt and A53T mice. In this study, A53T mice showed a reduced (S1-O) preference index observed at 3 (**$p < 0.01$; Fig. 1c3), 7 (***$p < 0.005$; Fig. 1c3), and 11 (***$p < 0.005$; Fig. 1c3) months of age. A reduction in the S2-S1 preference index was observed in 7- (*$p < 0.05$; Fig. 1d3) and 11-month-old (*,$p < 0.05$; Fig. 1d3) A53T mice as compared to their wt littermates. Finally, aging-induced changes in the S2-S1 preference index were detected between 3- and 11-month old A53T mice (**$p < 0.01$; Fig. 1d3).

### Expression of p-α-syn, GFAP, IBA1, Parvalbumin in mPFC

Earlier studies showed that overexpression of A53T mutant human α-syn in A53T mice causes impairment of neuronal function and neuronal toxicity [54, 55]. Observation of the mPFC of the A53T mice showed increased expression of p-α-syn in mPFC (***$p < 0.005$; Fig. 2g). Inflammation and astrogliosis are considered hallmarks of PD [56] and in A53T-related pathology [57–59]. The expression of GFAP, a marker of astrogliosis, was increased in A53T mice in the mPFC as compared to that in their age-matched controls (**$p < 0.01$; Fig. 2h). In the current study, increased IBA1 expression (*$p < 0.05$; Fig. 2i) and density of IBA1 positive cells (**$p < 0.01$; Fig. 2j) in the mPFC of the A53T mice was observed. Parvalbumin neurons (subpopulation of GABAergic interneurons) play an important role in social cognition [60–63]. Expression of parvalbumin (*$p < 0.05$; Fig. 3g), and number of parvalbumin positive cells were decreased in A53T mice (*$p < 0.05$; Fig. 3h).

### The Number of Orexin Neurons in LH

As mentioned above, α-syn is associated with neuronal function impairment and even death [54, 55]. Furthermore, there are strong indications that both orexin function impairment [23, 64] and orexin neuron loss are present in PD [24, 65]. As anticipated, p-α-syn aggregations were observed in orexin neurons. Although 53.12 ± 8.53 (mean ± SEM; Fig. 4d) of the orexin neurons contained p-α-syn aggregations, it did not affect the number of the orexin neurons in the LH (Fig. 4e), indicating an absence of orexin neuron loss in A53T mice at 7 months of age. However, reductions in orexin neuron numbers were observed in 11-month old A53T mice (7 months wt vs. 11 months A53T; **$p < 0.01$; 11 months wt vs. 11 months A53T; *$p < 0.05$).

### Pre-synaptic Inhibitory Terminal Quantification

Studies have identified GABA as a crucial factor in many processes regulated by the mPFC and in social cognition [66–68]. Quantification of pre-synaptic inhibitory terminals using an immunocytochemistry-based assay showed a reduction in the number of GAD65/synaptophysin co-localizations between wt mice and A53T mice at 7 months of age (*$p < 0.05$) (Fig. 5).

### Chemogenetic Manipulation of Orexin Neuron Activity

Prior to pursuing the chemogenetic studies, we addressed a recent report [69] indicating that CNO does not readily cross the blood-brain-barrier in vivo. Further, it was reported that CNO converts to clozapine in vivo, which has antipsychotic properties and may affect 3CSIT performance. Therefore, to exclude the possible independent actions of clozapine in our assay readouts, prior to the experiment described in Fig. 6, we performed elevated plus maze (EPM) and open field test (OFT) assays in orx-Cre cDREADD (control) mice to assess if CNO alone affected socialization and social memory. As shown in Fig. 6, there were no effects of CNO on either of these endpoints, suggesting that the conversion of CNO to clozapine does not affect the outcomes.

Studies show that orexin neurons are involved in regulation of the PFC, particularly mPFC function [31, 70, 71]. To test if chemogenetic modulation of orexin neuron activity can mitigate detected changes in social cognition parameters (socialization, social memory), we used a 3CSIT behavioral assay. Interestingly, social cognition of 7-month A53T mice was modulated by stimulation of orexin neurons. Compared to the control (orx-Cre) animals, orx-Cre/A53T mice showed reduced (S1-O) preference index in the 3CSIT (orx-Cre cDREADD CNO vs. orx-Cre/A53T cDREADD CNO; ***$p < 0.005$) (Fig. 7d3). DREADD-induced activation of orexin neurons in orx-Cre/A53T mice increased the S1-O index as compared to that of control mice (orx-Cre/A53T cDREADD CNO vs. orx-Cre/A53T qDREADD CNO; *$p < 0.05$) (Fig. 7d3). DREADD-induced inhibition of orexin neurons did not affect the S1-O preference index in 3CSIT; however, a difference was observed between the qDREADD and

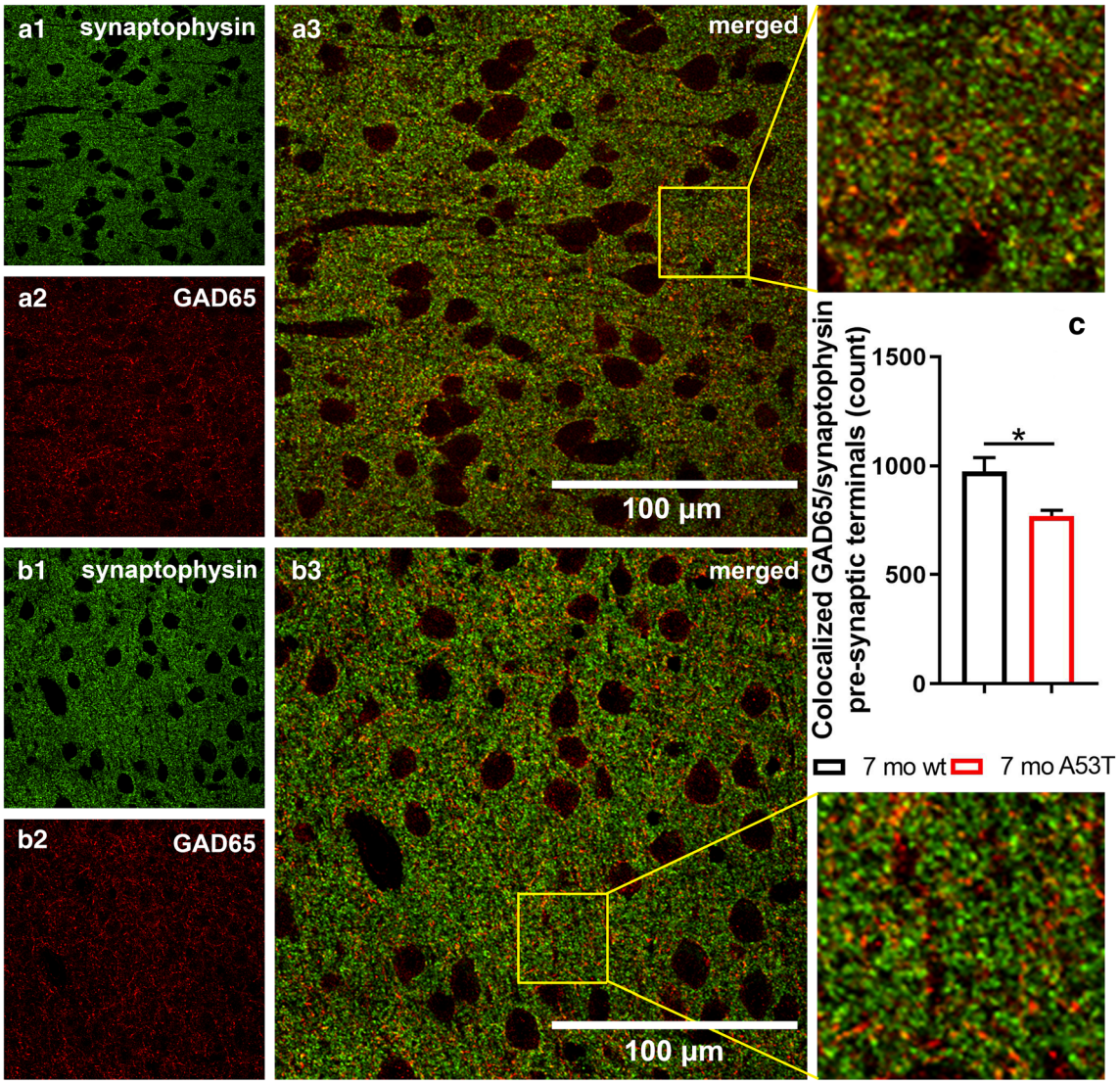


**Fig. 5** Quantification of inhibitory pre-synaptic terminals in 7-month-old wt and A53T mice. Representative high magnification IF microphotographs of the GAD65 and synaptophysin and merged images of the mPFC of 7-month wt mice (**a**) and A53T mice (**b**). Synaptophysin in green and GAD 65 in red. Immunocytochemistry-based assay showed reduced number of colocalized GAD65/synaptophysin pre-synaptic terminals in 7-month A53T mice compared to wt littermates. (Student's *t* test, $n = 3$/group; $*p < 0.05$)

iDREADD orx-Cre/A53T mice treated with CNO (orx-Cre/A53T qDREADD CNO vs. orx-Cre/A53T iDREADD CNO; $**p < 0.01$) (Fig. 7d3). Activation of orexin neurons also affected social memory. Compared to the control (orx-Cre) animals, orx-Cre/A53T mice showed reduced the S2-S1 preference index in the 3CSIT (orx-Cre cDREADD CNO vs. orx-Cre/A53T cDREADD CNO; $**p < 0.01$) (Fig. 7e3). Chemogenetic stimulation of orexin neurons in orx-Cre/A53T mice increased the S2-S1 index compared to that of control mice (orx-Cre/A53T cDREADD CNO vs. orx-Cre/A53T qDREADD CNO; $*p < 0.05$) (Fig. 7e3). Chemogenetic inhibition of orexin neurons did not affect the S2-S1 preference index in the 3CSIT; however, a difference was observed between the qDREADD and iDREADD orx-Cre/A53T mice treated with CNO (orx-Cre/A53T qDREADD CNO vs. orx-Cre/A53T iDREADD CNO; $**p < 0.01$) (Fig. 7e3).

## Confirmation of Injection Placement and DREADD Functionality

Orx-Cre/A53T mice used in the DREADD study received bilateral DREADD viral injections. Immunohistological analyses confirmed the selective expression of hM3Dq-mCherry in orexin neurons. Clear co-localization of orexin A and mCherry positive cells (OrxA/mCherry total mean ± SEM, cDREADD, 61.27 ± 5.01; qDREADD, 57.8 ± 6.88; iDREADD, 59.18 ± 7.27; Fig. 8d) were observed. Higher

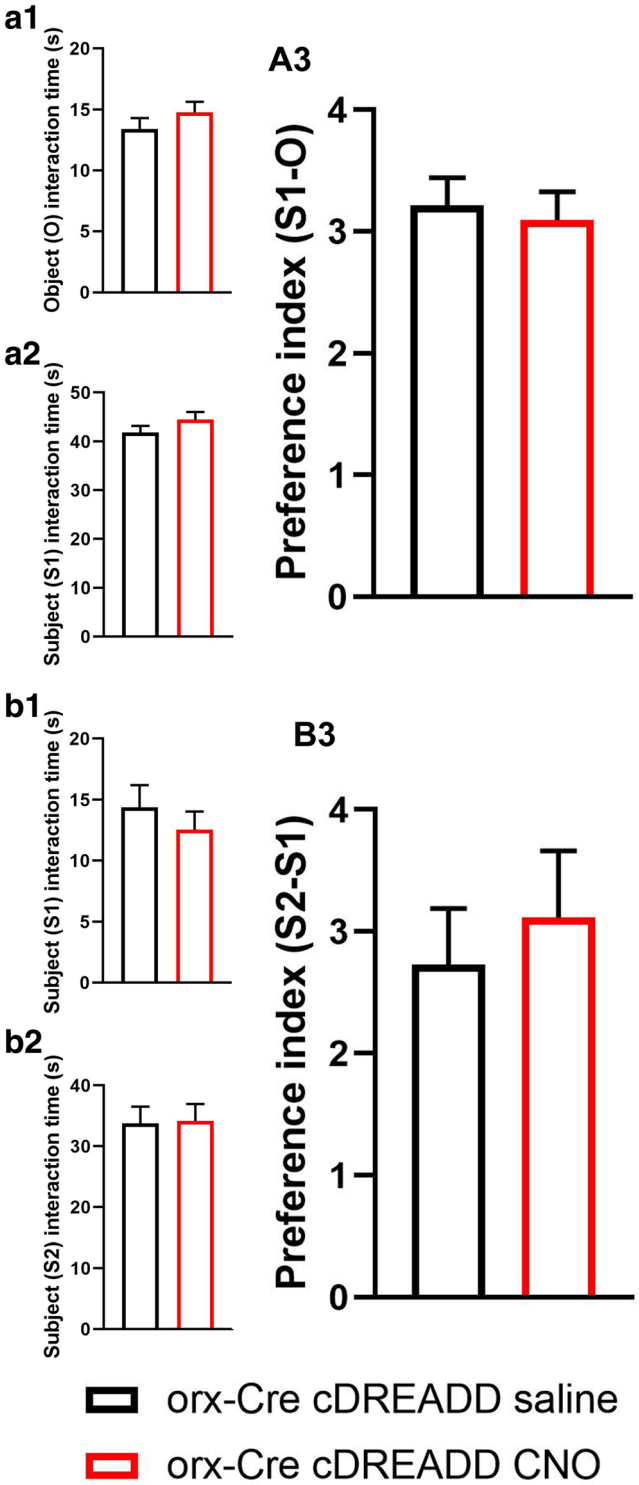


**Fig. 6** CNO effects on sociability and social memory in 7-month-old male mice. Sociability trials: time test mice spend interacting with empty cup (O) (**a1**), and stranger 1 (S1) mouse (**a2**). Compared to saline-treated mice, CNO-treated mice showed no difference in (S1-O) preference index (**a3**). Social memory trials: time test mice spend interacting with S1 (**b1**), and stranger 2 (S2) mouse (**b2**). No difference in (S2-S1) preference index between saline and CNO-treated animals were observed ($n = 6$/group; Student's $t$ test)

magnification images were used to estimate orexin neuronal specific expression of the immediate early gene, c-Fos. Measurement of c-Fos expression after CNO administration indicated that a majority of orexin neurons responded to CNO (OrxA/c-Fos CNO mean ± SEM, 71.42 ± 5.73) (Fig. 8d). The group of animals that received saline had minimal co-expression of orexin and c-Fos (OrxA/c-Fos saline mean ± SEM, 8.81 ± 1.80; Fig. 8d).

## Discussion

To our knowledge, we identified for the first time sociability and social memory impairment in the A53T mouse model of PD. We tested 3-, 7-, and 11-month-old A53T mice using the 3CSIT and detected early sociability impairments and progressive social memory loss. Several other PD mouse models show social memory impairment as well. A mouse model based on 6-hydroxydopamine (6-OHDA) toxin injection shows reductions in the capability of mice to discriminate between social odors, specifically self and non-self [72]. In MPTP (1-methyl-4-phenyl-1,2,3,6-tetrahydropyridine) models, decreases in social transmission of food preference [73] and social recognition impairments were observed [74]. Further, social cognition impairments were detected in the Thy1-aSyn model (mice overexpressing alpha-synuclein under the Thy1 promoter) mice [75]. Interestingly, Kurz et al. [76] show that overexpression of α-syn in A53T mice impairs dopamine signaling in striatum. This may be considered a contributing factor for social cognitive impairment given the significant role of dopamine in social cognition [77, 78] and the role of striatum in social behavior [29, 79]. In humans, several studies emphasize social cognitive deficits in PD patients. Systematic review of over one thousand patients using 16 different tests that assess sub-components of social cognition showed that PD patients suffer from social cognition impairments [39]. Another study observed low levels of empathy, impaired facial emotion, disorders in executive processing, poor performance in second-order and theory of mind tasks that assess both cognitive and affective processes [80]. Finally, social cognition impairments are observable in PD patients from early disease stages [39, 40] and pathological and functional changes in the PFC of PD patients [37, 38].

Following the behavioral experiments, we examined possible neuropathology in the mPFC of A53T mice. We observed α-syn accumulations and increases in IBA1 and GFAP expression and increases in IBA1 positive cells in the A53T mice. Overexpression of A53T mutant human α-syn in A53T mice increases neuronal toxicity and impairs neuronal function [54, 55]. Astrogliosis and inflammation are considered major factors in PD [56, 57], and astrogliosis and inflammation are involved in A53T-related pathology [57–59, 81]. Examination of cortex of A53T transgenic mice showed α-

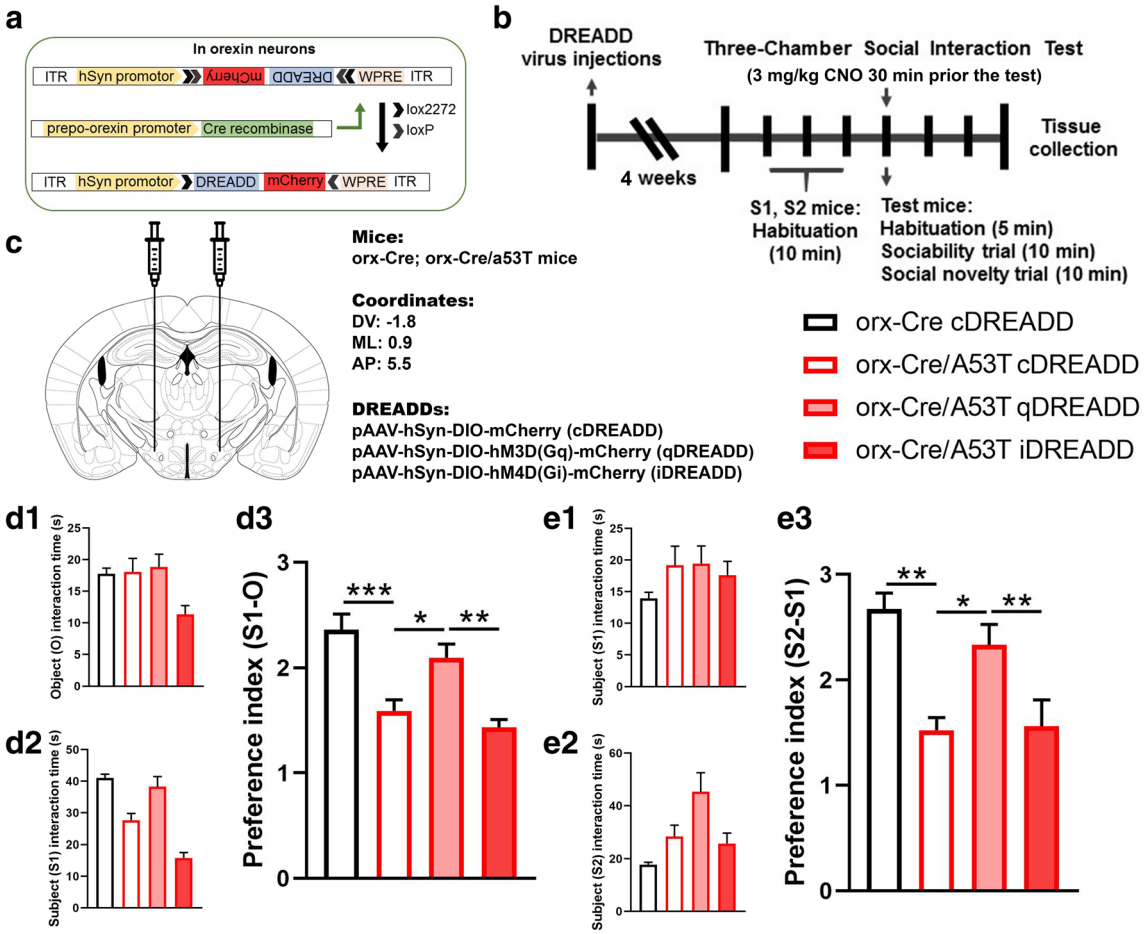


**Fig. 7** Chemogenetic modulation of sociability and social memory in 7-month-old A53T mice. Schematic diagram of AAV vector encoding DREADD-mCherry driven by human synapsin promoter (hSyn) promoter sequence and flanked by dual flox sites for recombination in the presence of Cre-recombinase (**a**). Cre expression in orx-Cre mice is driven by the prepro-orexin-promoter. The timeline of the experimental procedures. Orx-Cre and orx-Cre/A53T mice received intracranial viral injections (**b**). Orx-Cre mice received virus containing control DREADD construct, while orx-Cre/A53T mice received virus containing either control DREADD, excitatory DREADD or inhibitory DREADD construct. After 2 weeks of recovery time, 3CSIT was performed. Test mice were i.p. injected with 3 mg/kg of CNO dissolved in saline 30 min prior to the test. Three days following 3CSIT, mice were perfused and brains were collected. Schematic representation of DREADD virus injection site within the lateral hypothalamus (LH) (**c**). DREADD-virus constructs were injected bilaterally (333 nl/5 min). **d** Sociability trials. Time test mice spend interacting with empty cup (O) (**d1**), and stranger 1 (S1) mouse (**d2**). Compared to control (orx-Cre) mice orx-Cre/A53T mice showed increased (S1-O) preference index (**d3**). qDREADD activation of the orexin neurons increased (S1-O) preference index in orx-Cre/A53T mice (**d3**). iDREADD induced inhibition did not have a significant effect on the orx-Cre/A53T mice (**d3**). **e** Social memory trials. Time test mice spend interacting with S1 (**e1**), and stranger 2 (S2) mouse (**e2**). Compared to control (orx-Cre) mice, orx-Cre/A53T mice showed increased (S2-S1) preference index (**e3**). qDREADD activation of the orexin neurons increased (S2-S1) preference index in orx-Cre/A53T mice while iDREADD induced inhibition did not have a significant effect on the orx-Cre/A53T mice (**d3**). (orx-Cre with cDREADD, $n = 8$; orx-Cre/A53T with cDREADD, $n = 8$; orx-Cre/A53T with qDREADD, $n = 8$; orx-Cre/A53T with iDREADD, $n = 9$; two-way ANOVA, Sidak; $*p < 0.05$, $**p < 0.01$, $***p < 0.005$)

synuclein pathology and large detergent-insoluble aggregates of α-synuclein in both the frontal and cingulate cortex, also accompanied by features such as mitochondrial degeneration, lysosome pathology, and cell death [82, 83].

The observed behavioral phenotype (social cognitive disturbances) in A53T mice parallel changes observed in animals with GABA function impairment [84, 85]. Further, some studies emphasize the importance of parvalbumin neurons, a subpopulation of GABA neurons, in social cognition [60–63]. To assess whether A53T mice have GABA and parvalbumin-related impairments, we analyzed the number of GAD65 positive pre-synaptic terminals and the density of parvalbumin neurons in the mPFC. We detected a reduction in GAD65 pre-synaptic input and parvalbumin positive cell loss. Interestingly, the observed changes, both behavioral and biochemical, resemble alterations present in autism [86–88]. Moreover, high rates of PD are confirmed in people with autism spectrum disorders, and a recent study showed that *PARK2* (*parkin*, mutations of which are the second most common known cause of PD [89]) micro-duplication is associated with neurodevelopmental delay syndrome [90].

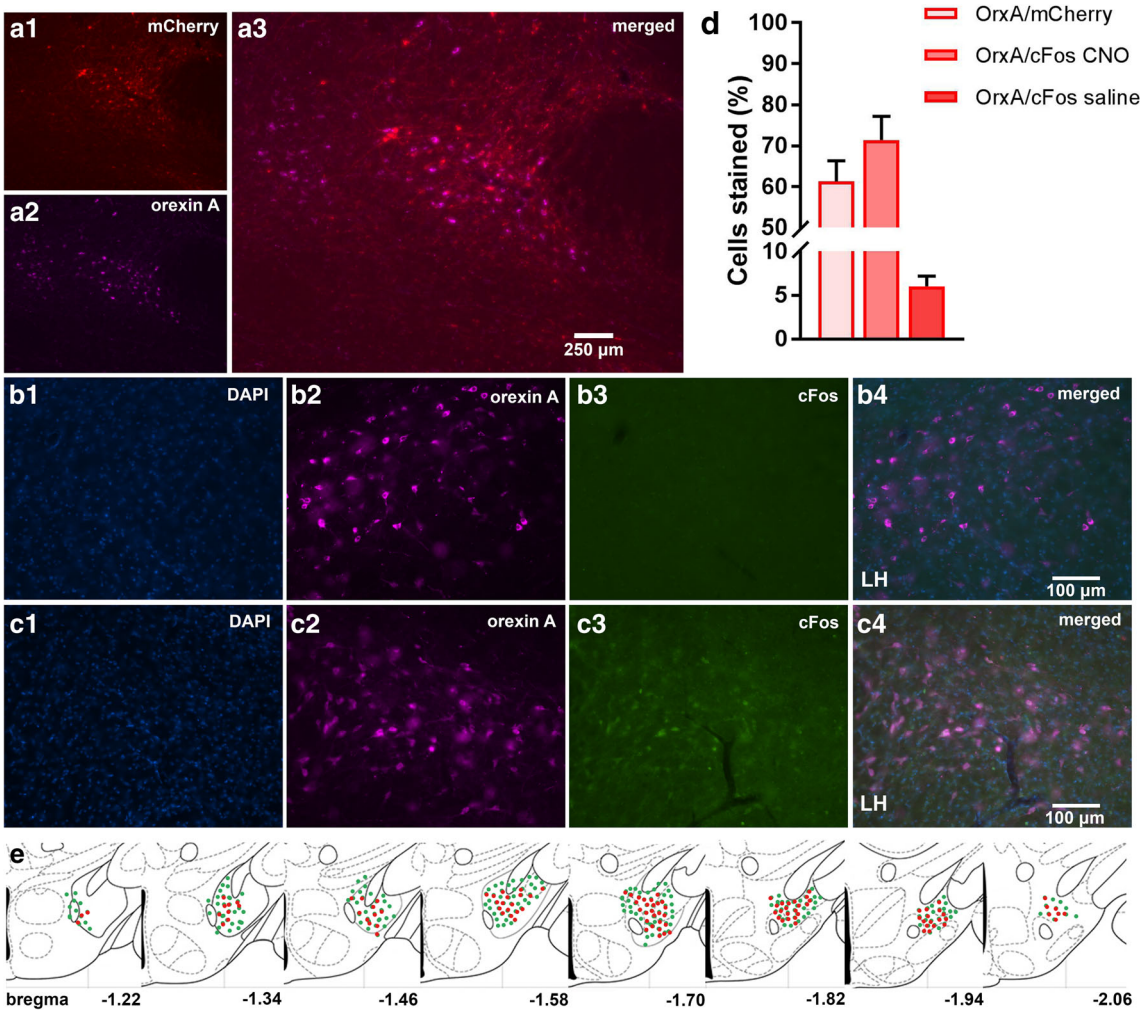


**Fig. 8** DREADD expression and functionality confirmation. Representative images displaying viral expression of DREADDs in the LH (**a**). mCherry positive neurons in red (**a1**), orexin A positive neurons in purple (**a2**), and merged images (**a3**). Representative images displaying c-Fos (early gene) expression. The LH of excitatory DREADD animals were treated with CNO 90 min prior to perfusion (**b**) and excitatory DREADD animals were treated with saline 90 min prior to perfusion (**c**). DAPI is shown in blue, orexin A is shown in purple, c-Fos in green, and then the merged images. The number of OrxA/mCherry and OrxA/c-Fos colocalized cells (**d**). Schematic drawings displaying the spread of viral expression along the LH; green orexin A expressing cells, red mCherry expressing cells (**e**) ($n = 5$/group)

Orexins play a significant role in PD pathology, and sleep disturbances in PD may be due to dysfunction of the orexin system [23, 91–94]. Further, reduced cerebrospinal fluid levels of orexin [95, 96] and loss of orexin neurons have been demonstrated in PD patients [24, 65]. In our study, we found α-syn accumulations in orexin neurons. Given the neurotoxic properties of α-syn [54, 55], we hypothesized that orexin neuron loss is present in A53T mice at 7 months of age. Although we found reduced numbers of orexin neurons, it was not statistically significant. We then hypothesized that the insignificant reduction in number of orexin neurons observed in A53T mice at 7 months of age could progress to significant neurodegeneration in 11-month-old A53T mice. As predicted, we observed orexin neuronal loss at 11 months of age in A53T mice (Fig. 4e).

The main goal of this study was to determine if in vivo modulation of orexin neuron activity could ameliorate sociability and social memory changes in A53Tmice. To achieve this, we used a chemogenetic approach. First, to address potential off-target effects of the designer ligand CNO [69], we performed the 3CSIT in orx-Cre cDREADD (control) mice. These studies confirmed that CNO treatment (3 mg/kg) did not have effects in control mice (Fig. 5), mitigating concern over off-target and independent effects of clozapine. To achieve chemogenetic modulation of orexin neurons, we created double transgenic orx-Cre/A53T mice, then intracranially injected them with virus containing either control, stimulatory or inhibitory DREADD constructs. After transfection, we subjected them to the 3CSIT behavioral assay. As hypothesized, we showed that chemogenetic activation of orexin neurons ameliorates social cognition impairments in A53T mice.

The main question arising from this study is how orexin neuronal modulation ameliorates social cognition impairment in A53T mice. It was previously shown that alterations of GABA interneuron function and impairment of inhibitory neurotransmission in PFC play a causal role in cognition as well as in stress-related neurobiological disorders [29, 97, 98]. Interestingly, orexin neuronal stimulation effects on social cognition in A53T mice could have been explained by the fact that orexin regulates glutamate input to fast-spiking interneurons in the PFC, causing the release of GABA [70]. It is possible that orexin chemogenetic intervention restores GABA system function and therefore ameliorates social cognition impairment. Considering the complex pattern of orexin projections, the observed effects of orexin neuron stimulation could have been indirect as well. This idea was not tested in the current study, but it merits future research.

There are neurobiological underpinnings of orexin action in the PFC: orexin receptors and fibers are present in the PFC, orexin projections emanate from LH to PFC, and studies show that orexin is a strong modulator of PFC function [7, 8, 31]. Orexin inputs can excite PFC neurons through both direct and indirect mechanisms inducing improvements in attention, short-term, and spatial memory [32–35]. Furthermore, acute intranasal administration of orexin A induces immediate early gene c-Fos expression, a marker for neuronal activation, and acetylcholine and glutamate release in the PFC [36]. Another study shows that orexin produces an increase in both GABA and glutamate release in PFC [70]. Finally, orexin selectively increases dopamine efflux within the prefrontal cortex [99], which is particularly interesting for PD research, considering the major dopamine system impairment present in this disease [100, 101].

## Conclusion

These data show that early social cognition impairment is present in the PD A53T mouse model, and early sociability disturbances are accompanied by progressive social memory loss. The PFC of A53T mice are affected by PD-related pathology, α-syn accumulation, inflammation, and astrogliosis. Further, GABA system impairment was shown by reduced GABA input and parvalbumin neuronal loss in the mPFC of A53T mice. Accumulations of α-syn in orexin neurons are accompanied by orexin cell loss at later stages of the disease (11-month-old mice), and activation of orexin neurons ameliorates PD related sociability and social memory impairments in A53T mice. These findings suggest that the A53T mouse may be an animal model of social cognitive impairment and GABA system disturbance in PD. Furthermore, these data implicate orexin neurons in PFC function consolidation and social cognition in the A53T PD mouse model and identify orexin as a potential therapeutic target for addressing early symptoms of PD.

**Acknowledgments** We would like to thank the Department of Neuroscience Mouse Behavior Core at the University of Minnesota for their support of the behavioral studies; the University of Minnesota Imaging Centers for their support of the confocal imaging; Dr. Chuanfeng Wang, MD, PhD from the Minneapolis VA Health Care System for providing the Stereo Investigator software and Axio Imager M2 fluorescence microscope; and Cagla Eroglu, PhD, Duke university for providing the Puncta Analyzer plugin for ImageJ software.

**Authors' Contribution** MS: conceived and designed research, performed experiments, analyzed data, interpreted results of experiments, prepared figures, drafted manuscript.

JPP: performed experiments, prepared figures.

AV: performed experiments, prepared figures.

CK: conceived and designed research, interpreted results of experiments, edited and revised manuscript, approved final version of manuscript.

**Funding** This work was supported by Department of Veterans Affairs (5I01RX000441-04 to CMK), the National Institute of Health (5R01DK100281-03).

## Compliance with Ethical Standards

**Conflict of Interest** The authors declare that they have no conflict of interest.

## References

1. Poewe W, Seppi K, Tanner CM, Halliday GM, Brundin P, Volkmann J, Schrag AE, Lang AE (2017) Parkinson disease. Nat Rev Dis Primer 3(17013). https://doi.org/10.1038/nrdp.2017.13
2. Kalia LV, Lang AE (2015) Parkinson's disease. Lancet 386:896–912. https://doi.org/10.1016/S0140-6736(14)61393-3
3. Anandhan A, Jacome MS, Lei S, Hernandez-Franco P, Pappa A, Panayiotidis MI, Powers R, Franco R (2017) Metabolic dysfunction in Parkinson's disease: Bioenergetics, redox homeostasis and central carbon metabolism. Brain Res Bull 133:12–30. https://doi.org/10.1016/j.brainresbull.2017.03.009
4. Tan LCS (2012) Mood disorders in Parkinson's disease. Parkinsonism Relat Disord 18:S74–S76. https://doi.org/10.1016/S1353-8020(11)70024-4
5. Davis AA, Racette B (2016) Parkinson disease and cognitive impairment. Neurol Clin Pract 6:452–458. https://doi.org/10.1212/CPJ.0000000000000285
6. Goldman JG, Litvan I (2011) Mild cognitive impairment in Parkinson's disease. Minerva Med 102:441–459
7. Sakurai T, Nagata R, Yamanaka A, Kawamura H, Tsujino N, Muraki Y, Kageyama H, Kunita S et al (2005) Input of orexin/hypocretin neurons revealed by a genetically encoded tracer in mice. Neuron 46:297–308. https://doi.org/10.1016/j.neuron.2005.03.010
8. Yoshida K, McCormack S, España RA, Crocker A, Scammell TE (2006) Afferents to the orexin neurons of the rat brain. J Comp Neurol 494:845–861. https://doi.org/10.1002/cne.20859
9. Girault EM, Yi C-X, Fliers E, Kalsbeek A (2012) Orexins, feeding, and energy balance. Prog Brain Res 198:47–64. https://doi.org/10.1016/B978-0-444-59489-1.00005-7

10. Tsujino N, Sakurai T (2009) Orexin/Hypocretin: A neuropeptide at the Interface of sleep, energy homeostasis, and reward system. Pharmacol Rev 61:162–176. https://doi.org/10.1124/pr.109.001321
11. Inutsuka A, Yamanaka A (2013) The physiological role of orexin/hypocretin neurons in the regulation of sleep/wakefulness and neuroendocrine functions. Front Endocrinol 4. https://doi.org/10.3389/fendo.2013.00018
12. De Lecea L, Huerta R (2014) Hypocretin (orexin) regulation of sleep-to-wake transitions. Front Pharmacol 5. https://doi.org/10.3389/fphar.2014.00016
13. Kotz CM (2006) Integration of feeding and spontaneous physical activity: Role for orexin. Physiol Behav 88:294–301. https://doi.org/10.1016/j.physbeh.2006.05.031
14. Perez-Leighton CE, Little MR, Grace MK, Billington C, Kotz CM (2016) Orexin signaling in rostral lateral hypothalamus and nucleus accumbens shell in the control of spontaneous physical activity in high and low activity rats. Am J Physiol - Regul Integr Comp Physiol ajpregu 312:R338–R346. https://doi.org/10.1152/ajpregu.00339.2016
15. Johnson PL, Molosh A, Fitz SD et al (2012) Orexin, stress, and anxiety/panic states. Prog Brain Res 198:133–161. https://doi.org/10.1016/B978-0-444-59489-1.00009-4
16. Yeoh JW, Campbell EJ, James MH, Graham BA, Dayas CV (2014) Orexin antagonists for neuropsychiatric disease: Progress and potential pitfalls. Front Neurosci 8. https://doi.org/10.3389/fnins.2014.00036
17. Muschamp JW, Hollander JA, Thompson JL, Voren G, Hassinger LC, Onvani S, Kamenecka TM, Borgland SL et al (2014) Hypocretin (orexin) facilitates reward by attenuating the antireward effects of its cotransmitter dynorphin in ventral tegmental area. Proc Natl Acad Sci 111:E1648–E1655. https://doi.org/10.1073/pnas.1315542111
18. Mavanji V, Butterick TA, Duffy CM, Nixon JP, Billington CJ, Kotz CM (2017) Orexin/hypocretin treatment restores hippocampal-dependent memory in orexin-deficient mice. Neurobiol Learn Mem 146:21–30. https://doi.org/10.1016/j.nlm.2017.10.014
19. Flores Á, Valls-Comamala V, Costa G, Saravia R, Maldonado R, Berrendero F (2014) The Hypocretin/orexin system mediates the extinction of fear memories. Neuropsychopharmacology 39:2732–2741. https://doi.org/10.1038/npp.2014.146
20. James MH, Campbell EJ, Dayas CV (2017) Role of the orexin/Hypocretin system in stress-related psychiatric disorders. Curr Top Behav Neurosci 33:197–219. https://doi.org/10.1007/7854_2016_56
21. Razavi BM, Hosseinzadeh H (2017) A review of the role of orexin system in pain modulation. Biomed Pharmacother Biomedecine Pharmacother 90:187–193. https://doi.org/10.1016/j.biopha.2017.03.053
22. Bridoux A, Moutereau S, Covali-Noroc A et al (2013) Ventricular orexin-a (hypocretin-1) levels correlate with rapid-eye-movement sleep without atonia in Parkinson's disease. Nat Sci Sleep 5:87–91. https://doi.org/10.2147/NSS.S41245
23. Baumann CR, Scammell TE, Bassetti CL (2008) Parkinson's disease, sleepiness and hypocretin/orexin. Brain J Neurol 131:e91. https://doi.org/10.1093/brain/awm220
24. Thannickal TC, Lai Y-Y, Siegel JM (2007) Hypocretin (orexin) cell loss in Parkinson's disease. Brain J Neurol 130:1586–1595. https://doi.org/10.1093/brain/awm097
25. Fronczek R, van Geest S, Frölich M, Overeem S, Roelandse FWC, Lammers GJ, Swaab DF (2012) Hypocretin (orexin) loss in Alzheimer's disease. Neurobiol Aging 33:1642–1650. https://doi.org/10.1016/j.neurobiolaging.2011.03.014
26. Wood JN (2003) Social cognition and the prefrontal cortex. Behav Cogn Neurosci Rev 2:97–114. https://doi.org/10.1177/1534582303002002002
27. Amodio DM, Frith CD (2006) Meeting of minds: The medial frontal cortex and social cognition. Nat Rev Neurosci 7:268–277. https://doi.org/10.1038/nrn1884
28. Zaki J, Hennigan K, Weber J, Ochsner KN (2010) Social cognitive conflict resolution: Contributions of domain general and domain specific neural systems. J Neurosci 30:8481–8488. https://doi.org/10.1523/JNEUROSCI.0382-10.2010
29. Bicks LK, Koike H, Akbarian S, Morishita H (2015) Prefrontal cortex and social cognition in mouse and man. Front Psychol 6. https://doi.org/10.3389/fpsyg.2015.01805
30. Lieberman MD (2007) Social cognitive neuroscience: A review of core processes. Annu Rev Psychol 58:259–289. https://doi.org/10.1146/annurev.psych.58.110405.085654
31. Jin J, Chen Q, Qiao Q, Yang L, Xiong J, Xia J, Hu Z, Chen F (2016) Orexin neurons in the lateral hypothalamus project to the medial prefrontal cortex with a rostro-caudal gradient. Neurosci Lett 621:9–14. https://doi.org/10.1016/j.neulet.2016.04.002
32. Lambe EK, Aghajanian GK (2003) Hypocretin (orexin) induces calcium transients in single spines postsynaptic to identified thalamocortical boutons in prefrontal slice. Neuron 40:139–150
33. Lee MG, Hassani OK, Jones BE (2005) Discharge of identified orexin/hypocretin neurons across the sleep-waking cycle. J Neurosci 25:6716–6720. https://doi.org/10.1523/JNEUROSCI.1887-05.2005
34. Xia J, Chen X, Song C, Ye J, Yu Z, Hu Z (2005) Postsynaptic excitation of prefrontal cortical pyramidal neurons by hypocretin-1/orexin a through the inhibition of potassium currents. J Neurosci Res 82:729–736. https://doi.org/10.1002/jnr.20667
35. Aitta-aho T, Pappa E, Burdakov D, Apergis-Schoute J (2016) Cellular activation of hypothalamic hypocretin/orexin neurons facilitates short-term spatial memory in mice. Neurobiol Learn Mem 136:183–188. https://doi.org/10.1016/j.nlm.2016.10.005
36. Calva CB, Fayyaz H, Fadel JR (2018) Increased acetylcholine and glutamate efflux in the prefrontal cortex following intranasal orexin-a (hypocretin-1). J Neurochem 145:232–244. https://doi.org/10.1111/jnc.14279
37. Prakash KG, Bannur BM, Chavan MD, Saniya K, Sailesh KS, Rajagopalan A (2016) Neuroanatomical changes in Parkinson's disease in relation to cognition: An update. J Adv Pharm Technol Res 7:123–126. https://doi.org/10.4103/2231-4040.191416
38. Kendi ATK, Lehericy S, Luciana M et al (2008) Altered diffusion in the frontal lobe in Parkinson disease. Am J Neuroradiol 29:501–505. https://doi.org/10.3174/ajnr.A0850
39. Palmeri R, Lo Buono V, Corallo F, Foti M, di Lorenzo G, Bramanti P, Marino S (2017) Nonmotor symptoms in Parkinson disease: A descriptive review on social cognition ability. J Geriatr Psychiatry Neurol 30:109–121. https://doi.org/10.1177/0891988716687872
40. Yoshimura N, Kawamura M (2005) Impairment of social cognition in Parkinson's disease. No To Shinkei 57:107–113
41. Dawson TM, Ko HS, Dawson VL (2010) Genetic animal models of Parkinson's disease. Neuron 66:646–661. https://doi.org/10.1016/j.neuron.2010.04.034
42. Paumier KL, Rizzo SJS, Berger Z et al (2013) Behavioral characterization of A53T mice reveals early and late stage deficits related to Parkinson's disease. PLoS One 8:e70274. https://doi.org/10.1371/journal.pone.0070274
43. Lee MK, Stirling W, Xu Y, Xu X, Qui D, Mandir AS, Dawson TM, Copeland NG et al (2002) Human α-synuclein-harboring familial Parkinson's disease-linked ala-53 → Thr mutation causes neurodegenerative disease with α-synuclein aggregation in

transgenic mice. Proc Natl Acad Sci U S A 99:8968–8973. https://doi.org/10.1073/pnas.132197599
44. Farrell KF, Krishnamachari S, Villanueva E, Lou H, Alerte TNM, Peet E, Drolet RE, Perez RG (2014) Non-motor parkinsonian pathology in aging A53T α-Synuclein mice is associated with progressive synucleinopathy and altered enzymatic function. J Neurochem 128:536–546. https://doi.org/10.1111/jnc.12481
45. Graham DR, Sidhu A (2010) Mice expressing the A53T mutant form of human alpha-Synuclein exhibit hyperactivity and reduced anxiety-like behavior. J Neurosci Res 88:1777–1783. https://doi.org/10.1002/jnr.22331
46. Unger EL, Eve DJ, Perez XA, Reichenbach DK, Xu Y, Lee MK, Andrews AM (2006) Locomotor hyperactivity and alterations in dopamine neurotransmission are associated with overexpression of A53T mutant human alpha-synuclein in mice. Neurobiol Dis 21:431–443. https://doi.org/10.1016/j.nbd.2005.08.005
47. Matsuki T, Nomiyama M, Takahira H, Hirashima N, Kunita S, Takahashi S, Yagami KI, Kilduff TS et al (2009) Selective loss of GABA(B) receptors in orexin-producing neurons results in disrupted sleep/wakefulness architecture. Proc Natl Acad Sci U S A 106:4459–4464. https://doi.org/10.1073/pnas.0811126106
48. Zink AN, Bunney PE, Holm AA, Billington CJ, Kotz CM (2005) (2018) neuromodulation of orexin neurons reduces diet-induced adiposity. Int J Obes 42:737–745. https://doi.org/10.1038/ijo.2017.276
49. Giasson BI, Duda JE, Quinn SM, Zhang B, Trojanowski JQ, Lee VMY (2002) Neuronal α-Synucleinopathy with severe movement disorder in mice expressing A53T human α-Synuclein. Neuron 34:521–533. https://doi.org/10.1016/S0896-6273(02)00682-7
50. Franklin K (2008) The mouse brain in stereotaxic coordinates. Acad. Press **Amsterdam] [u.a.**
51. McKinstry SU, Karadeniz YB, Worthington AK et al (2014) Huntingtin is required for Normal excitatory synapse development in cortical and striatal circuits. J Neurosci 34:9455–9472. https://doi.org/10.1523/JNEUROSCI.4699-13.2014
52. Ippolito DM, Eroglu C (2010) Quantifying synapses: An immunocytochemistry-based assay to quantify synapse number. J Vis Exp JoVE. https://doi.org/10.3791/2270
53. Franklin KBJ, Paxinos G (2008) The mouse brain in stereotaxic coordinates
54. Lee S, Oh ST, Jeong HJ, Pak SC, Park HJ, Kim J, Cho HS, Jeon S (2017) MPTP-induced vulnerability of dopamine neurons in A53T α-synuclein overexpressed mice with the potential involvement of DJ-1 downregulation. Korean J Physiol Pharmacol Off J Korean Physiol Soc Korean Soc Pharmacol 21:625–632. https://doi.org/10.4196/kjpp.2017.21.6.625
55. Xie Z, Turkson S, Zhuang X (2015) A53T human α-Synuclein overexpression in transgenic mice induces pervasive mitochondria macroautophagy defects preceding dopamine neuron degeneration. J Neurosci 35:890–905. https://doi.org/10.1523/JNEUROSCI.0089-14.2015
56. Phani S, Loike JD, Przedborski S (2012) Neurodegeneration and inflammation in Parkinson's disease. Parkinsonism Relat Disord 18:S207–S209. https://doi.org/10.1016/S1353-8020(11)70064-5
57. Booth HDE, Hirst WD, Wade-Martins R (2017) The role of astrocyte dysfunction in Parkinson's disease pathogenesis. Trends Neurosci 40:358–370. https://doi.org/10.1016/j.tins.2017.04.001
58. Fellner L, Jellinger KA, Wenning GK, Stefanova N (2011) Glial dysfunction in the pathogenesis of α-synucleinopathies: Emerging concepts. Acta Neuropathol (Berl) 121:675–693. https://doi.org/10.1007/s00401-011-0833-z
59. Gu X-L, Long C-X, Sun L, Xie C, Lin X, Cai H (2010) Astrocytic expression of Parkinson's disease-related A53T α-synuclein causes neurodegeneration in mice. Mol Brain 3:12. https://doi.org/10.1186/1756-6606-3-12
60. Murray AJ, Woloszynowska-Fraser MU, Ansel-Bollepalli L, Cole KLH, Foggetti A, Crouch B, Riedel G, Wulff P (2015) Parvalbumin-positive interneurons of the prefrontal cortex support working memory and cognitive flexibility. Sci Rep 5:16778. https://doi.org/10.1038/srep16778
61. Chen C-C, Lu J, Yang R, Ding JB, Zuo Y (2018) Selective activation of parvalbumin interneurons prevents stress-induced synapse loss and perceptual defects. Mol Psychiatry 23:1614–1625. https://doi.org/10.1038/mp.2017.159
62. Wöhr M, Orduz D, Gregory P, Moreno H, Khan U, Vörckel KJ, Wolfer DP, Welzl H et al (2015) Lack of parvalbumin in mice leads to behavioral deficits relevant to all human autism core symptoms and related neural morphofunctional abnormalities. Transl Psychiatry 5:e525. https://doi.org/10.1038/tp.2015.19
63. Yizhar O, Fenno LE, Prigge M, Schneider F, Davidson TJ, O'Shea DJ, Sohal VS, Goshen I et al (2011) Neocortical excitation/inhibition balance in information processing and social dysfunction. Nature 477:171–178. https://doi.org/10.1038/nature10360
64. Takahashi Y, Kanbayashi T, Hoshikawa M, Imanishi A, Sagawa Y, Tsutsui K, Takeda Y, Kusanagi H et al (2015) Relationship of orexin (hypocretin) system and astrocyte activation in Parkinson's disease with hypersomnolence. Sleep Biol Rhythms 13:252–260. https://doi.org/10.1111/sbr.12112
65. Fronczek R, Overeem S, Lee SYY, Hegeman IM, van Pelt J, van Duinen SG, Lammers GJ, Swaab DF (2007) Hypocretin (orexin) loss in Parkinson's disease. Brain J Neurol 130:1577–1585. https://doi.org/10.1093/brain/awm090
66. Delli Pizzi S, Chiacchiaretta P, Mantini D, Bubbico G, Edden RA, Onofrj M, Ferretti A, Bonanni L (2017) GABA content within medial prefrontal cortex predicts the variability of fronto-limbic effective connectivity. Brain Struct Funct 222:3217–3229. https://doi.org/10.1007/s00429-017-1399-x
67. Bañuelos C, Beas BS, McQuail JA et al (2014) Prefrontal cortical GABAergic dysfunction contributes to age-related working memory impairment. J Neurosci 34:3457–3466. https://doi.org/10.1523/JNEUROSCI.5192-13.2014
68. Houtepen LC, Schür RR, Wijnen JP, Boer VO, Boks MPM, Kahn RS, Joëls M, Klomp DW et al (2017) Acute stress effects on GABA and glutamate levels in the prefrontal cortex: A 7T 1H magnetic resonance spectroscopy study. NeuroImage Clin 14:195–200. https://doi.org/10.1016/j.nicl.2017.01.001
69. Gomez JL, Bonaventura J, Lesniak W, Mathews WB, Sysa-Shah P, Rodriguez LA, Ellis RJ, Richie CT et al (2017) Chemogenetics revealed: DREADD occupancy and activation via converted clozapine. Science 357:503–507. https://doi.org/10.1126/science.aan2475
70. Aracri P, Banfi D, Pasini ME, Amadeo A, Becchetti A (2015) Hypocretin (orexin) regulates glutamate input to fast-spiking interneurons in layer V of the Fr2 region of the murine prefrontal cortex. Cereb Cortex N Y NY 25:1330–1347. https://doi.org/10.1093/cercor/bht326
71. Xia JX, Fan SY, Yan J, Chen F, Li Y, Yu ZP, Hu ZA (2009) Orexin A-induced extracellular calcium influx in prefrontal cortex neurons involves L-type calcium channels. J Physiol Biochem 65:125–136. https://doi.org/10.1007/BF03179063
72. Bonito-Oliva A, Masini D, Fisone G (2014) A mouse model of non-motor symptoms in Parkinson's disease: Focus on pharmacological interventions targeting affective dysfunctions. Front Behav Neurosci 8. https://doi.org/10.3389/fnbeh.2014.00290
73. Vucković MG, Wood RI, Holschneider DP et al (2008) Memory, mood, dopamine, and serotonin in the 1-methyl-4-phenyl-1,2,3,6-tetrahydropyridine-lesioned mouse model of basal ganglia injury. Neurobiol Dis 32:319–327. https://doi.org/10.1016/j.nbd.2008.07.015

74. Doty RL, Singh A, Tetrud J, Langston JW (1992) Lack of major olfactory dysfunction in MPTP-induced parkinsonism. Ann Neurol 32:97–100. https://doi.org/10.1002/ana.410320116
75. Magen I, Torres ER, Dinh D, Chung A, Masliah E, Chesselet MF (2015) Social cognition impairments in mice overexpressing alpha-Synuclein under the Thy1 promoter, a model of pre-manifest Parkinson's disease. J Park Dis 5:669–680. https://doi.org/10.3233/JPD-140503
76. Kurz A, Double KL, Lastres-Becker I, Tozzi A, Tantucci M, Bockhart V, Bonin M, García-Arencibia M et al (2010) A53T-alpha-Synuclein overexpression impairs dopamine signaling and striatal synaptic plasticity in old mice. PLoS One 5:e11464. https://doi.org/10.1371/journal.pone.0011464
77. Homberg JR, Olivier JDA, VandenBroeke M, Youn J, Ellenbroek AK, Karel P, Shan L, van Boxtel R et al (2016) The role of the dopamine D1 receptor in social cognition: Studies using a novel genetic rat model. Dis Model Mech 9:1147–1158. https://doi.org/10.1242/dmm.024752
78. Gunaydin LA, Deisseroth K (2014) Dopaminergic dynamics contributing to social behavior. Cold Spring Harb Symp Quant Biol 79:221–227. https://doi.org/10.1101/sqb.2014.79.024711
79. Báez-Mendoza R, Schultz W (2013) The role of the striatum in social behavior. Front Neurosci 7. https://doi.org/10.3389/fnins.2013.00233
80. Narme P, Mouras H, Roussel M, Duru C, Krystkowiak P, Godefroy O (2013) Emotional and cognitive social processes are impaired in Parkinson's disease and are related to behavioral disorders. Neuropsychology 27:182–192. https://doi.org/10.1037/a0031522
81. Hoenen C, Gustin A, Birck C, Kirchmeyer M, Beaume N, Felten P, Grandbarbe L, Heuschling P et al (2016) Alpha-Synuclein proteins promote pro-inflammatory cascades in microglia: Stronger effects of the A53T mutant. PLoS One 11:e0162717. https://doi.org/10.1371/journal.pone.0162717
82. Martin LJ, Pan Y, Price AC, Sterling W, Copeland NG, Jenkins NA, Price DL, Lee MK (2006) Parkinson's disease α-Synuclein transgenic mice develop neuronal mitochondrial degeneration and cell death. J Neurosci 26:41–50. https://doi.org/10.1523/JNEUROSCI.4308-05.2006
83. Rockenstein E, Schwach G, Ingolic E, Adame A, Crews L, Mante M, Pfragner R, Schreiner E et al (2005) Lysosomal pathology associated with alpha-synuclein accumulation in transgenic models using an eGFP fusion protein. J Neurosci Res 80:247–259. https://doi.org/10.1002/jnr.20446
84. Paine TA, Swedlow N, Swetschinski L (2017) Decreasing GABA function within the medial prefrontal cortex or basolateral amygdala decreases sociability. Behav Brain Res 317:542–552. https://doi.org/10.1016/j.bbr.2016.10.012
85. Kolata SM, Nakao K, Jeevakumar V, Farmer-Alroth EL, Fujita Y, Bartley AF, Jiang SZ, Rompala GR et al (2018) Neuropsychiatric phenotypes produced by GABA reduction in mouse cortex and hippocampus. Neuropsychopharmacol Off Publ Am Coll Neuropsychopharmacol 43:1445–1456. https://doi.org/10.1038/npp.2017.296
86. Hashemi E, Ariza J, Rogers H, Noctor SC, Martínez-Cerdeño V (1991) (2017) the number of Parvalbumin-expressing interneurons is decreased in the prefrontal cortex in autism. Cereb Cortex N Y N 27:1931–1943. https://doi.org/10.1093/cercor/bhw021
87. Villalobos CA, Wu Q, Lee PH, May PJ, Basso MA (2018) Parvalbumin and GABA microcircuits in the mouse superior colliculus. Front Neural Circuits 12. https://doi.org/10.3389/fncir.2018.00035
88. Leekam S (2016) Social cognitive impairment and autism: what are we trying to explain? Philos Trans R Soc B Biol Sci 371:20150082. https://doi.org/10.1098/rstb.2015.0082
89. Dawson TM, Dawson VL (2010) The role of Parkin in familial and sporadic Parkinson's disease. Mov Disord Off J Mov Disord Soc 25:S32–S39. https://doi.org/10.1002/mds.22798
90. Palumbo O, Palumbo P, Leone MP, Stallone R, Palladino T, Vendemiale M, Palladino S, Papadia F et al (2016) PARK2 microduplication: Clinical and molecular characterization of a further case and review of the literature. Mol Syndromol 7:282–286. https://doi.org/10.1159/000448852
91. Compta Y, Santamaria J, Ratti L, Tolosa E, Iranzo A, Munoz E, Valldeoriola F, Casamitjana R et al (2009) Cerebrospinal hypocretin, daytime sleepiness and sleep architecture in Parkinson's disease dementia. Brain J Neurol 132:3308–3317. https://doi.org/10.1093/brain/awp263
92. Asai H, Hirano M, Furiya Y, Udaka F, Morikawa M, Kanbayashi T, Shimizu T, Ueno S (2009) Cerebrospinal fluid-orexin levels and sleep attacks in four patients with Parkinson's disease. Clin Neurol Neurosurg 111:341–344. https://doi.org/10.1016/j.clineuro.2008.11.007
93. Dhawan V, Healy DG, Pal S, Chaudhuri KR (2006) Sleep-related problems of Parkinson's disease. Age Ageing 35:220–228. https://doi.org/10.1093/ageing/afj087
94. Abbott RD, Ross GW, White LR, Tanner CM, Masaki KH, Nelson JS, Curb JD, Petrovitch H (2005) Excessive daytime sleepiness and subsequent development of Parkinson disease. Neurology 65:1442–1446. https://doi.org/10.1212/01.wnl.0000183056.89590.0d
95. Drouot X, Moutereau S, Nguyen JP, Lefaucheur JP, Creange A, Remy P, Goldenberg F, d'Ortho MP (2003) Low levels of ventricular CSF orexin/hypocretin in advanced PD. Neurology 61:540–543
96. Yasui K, Inoue Y, Kanbayashi T, Nomura T, Kusumi M, Nakashima K (2006) CSF orexin levels of Parkinson's disease, dementia with Lewy bodies, progressive supranuclear palsy and corticobasal degeneration. J Neurol Sci 250:120–123. https://doi.org/10.1016/j.jns.2006.08.004
97. Auger ML, Floresco SB (2014) Prefrontal cortical GABA modulation of spatial reference and working memory. Int J Neuropsychopharmacol 18. https://doi.org/10.1093/ijnp/pyu013
98. Ghosal S, Hare B, Duman RS (2017) Prefrontal cortex GABAergic deficits and circuit dysfunction in the pathophysiology and treatment of chronic stress and depression. Curr Opin Behav Sci 14:1–8. https://doi.org/10.1016/j.cobeha.2016.09.012
99. Calipari ES, España RA (2012) Hypocretin/orexin regulation of dopamine signaling: Implications for reward and reinforcement mechanisms. Front Behav Neurosci 6. https://doi.org/10.3389/fnbeh.2012.00054
100. Surmeier DJ (2018) Determinants of dopaminergic neuron loss in Parkinson's disease. FEBS J 285:3657–3668. https://doi.org/10.1111/febs.14607
101. Isaias IU, Trujillo P, Summers P, Marotta G, Mainardi L, Pezzoli G, Zecca L, Costa A (2016) Neuromelanin imaging and dopaminergic loss in Parkinson's disease. Front Aging Neurosci 8. https://doi.org/10.3389/fnagi.2016.00196